

Article

Validation of Voltammetric Methods for Online Analysis of Platinum Dissolution in a Hydrogen PEM Fuel Cell Stack

Lena Birkner  and Maik Eichelbaum * 

Department of Applied Chemistry, Georg Simon Ohm University of Applied Sciences Nuremberg, Prinzregentenauer 47, 90489 Nuremberg, Germany

* Correspondence: maik.eichelbaum@th-nuernberg.de; Tel.: +49-911-5880-1561

Abstract: Platinum dissolution in PEM fuel cells is an increasingly important indicator for the state-of-health and lifetime prediction of fuel cells in real applications. For this reason, portable online analysis tools are needed that can detect and quantify platinum with high sensitivity, selectivity, and accuracy in the product water of fuel cells. We validated the hanging mercury drop electrode (HMDE) and non-toxic bismuth film electrodes for the voltammetric determination of platinum for this purpose. Bismuth films were prepared by reductive deposition on both a glassy carbon solid state electrode and on a screen-printed electrode (film on-chip electrode). Both bismuth film electrodes could be successfully validated for the determination of platinum by adsorptive stripping voltammetry. An LOD of 7.9 $\mu\text{g/L}$ and an LOQ of 29.1 $\mu\text{g/L}$ were determined for the bismuth film solid state electrode, values of 22.5 $\mu\text{g/L}$ for the LOD and of 79.0 $\mu\text{g/L}$ for the LOQ were obtained for the bismuth film on-chip electrode. These numbers are still much higher than the results measured with the HMDE (LOD: 0.76 ng/L ; LOQ: 2.8 ng/L) and are not sufficient to detect platinum in the product water of a fuel cell run in different load tests. The amount of dissolved platinum produced by a 100 W fuel cell stack upon dynamic and continuous high load cycling, respectively, was in the range of 2.9–4.1 ng/L , which could only be detected by the HMDE.



Citation: Birkner, L.; Eichelbaum, M. Validation of Voltammetric Methods for Online Analysis of Platinum Dissolution in a Hydrogen PEM Fuel Cell Stack. *Electrochem* **2022**, *3*, 728–745. <https://doi.org/10.3390/electrochem3040048>

Academic Editor: Masato Sone

Received: 19 September 2022

Accepted: 28 October 2022

Published: 7 November 2022

Publisher's Note: MDPI stays neutral with regard to jurisdictional claims in published maps and institutional affiliations.



Copyright: © 2022 by the authors. Licensee MDPI, Basel, Switzerland. This article is an open access article distributed under the terms and conditions of the Creative Commons Attribution (CC BY) license (<https://creativecommons.org/licenses/by/4.0/>).

Keywords: hanging mercury drop electrode; bismuth film electrode; screen-printed electrode; on-chip sensor; PEM fuel cell; platinum dissolution; online analysis tool; adsorptive stripping voltammetry; high load and dynamic load cycling

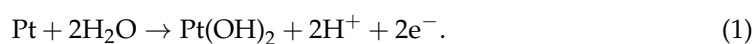
1. Introduction

With the breakthrough experiments made by Jaroslav Heyrovský in the 1920s, the dropping mercury electrode has become the most important working electrode for the ultratrace determination of metals in aqueous samples by voltammetric measurements [1]. Mercury has many advantages such as a high overpotential for molecular hydrogen formation, enabling measurements at very negative potentials. It is ideally polarizable and has given the entire field of voltammetry with (liquid) mercury drop electrodes the name polarography. Moreover, with every new drop a perfectly new surface is formed avoiding the typical deactivation observed for solid state electrodes after several uses, and finally, the formation of amalgams makes the reduction of many metal species thermodynamically more favorable. Unfortunately, mercury is highly toxic. It is a liquid at room temperature and has a fairly high vapor pressure for a metal. Exposure to mercury or mercury vapor can cause severe damages to the brain, kidneys, and lungs. It is also responsible for severe diseases such as acrodynia, Hunter–Russell syndrome, and Minamata disease [2]. Unfortunately, there are nearly no treatments for acute and long-term mercury poisoning. Emissions, and the use and disposal of mercury is therefore strictly regulated in most countries. E.g., the European Union limited or even banned the usage of mercury in several applications and devices [3]. Moreover, the Minamata Convention on Mercury, ratified by 140 countries, comprises an international treaty to protect human health and the environment from anthropogenic emissions and releases of mercury and mercury compounds [4].

As a consequence, the voltammetric community is looking desperately for non-, or at least less, toxic alternatives that can replace mercury in most voltammetric applications. Many tested materials failed due to a low cathodic potential limit, high background noise, lack of reproducibility or multiple peak formation in the voltammogram. More than two decades ago, bismuth coated electrodes were considered for the first time to determine zinc, cadmium, and lead by anodic stripping voltammetry [5,6]. Bismuth films on glassy carbon and carbon fiber electrodes, respectively, have been successfully tested, which are formed in situ together with the enrichment of the analyte in the film electrode. Bismuth provides an accessible potential window between approximately -0.2 and -1.2 V (versus Ag/AgCl), which is restricted by hydrogen formation on the cathodic side and by bismuth oxidation on the anodic side. Due to this broad potential window very similar to mercury, a simultaneous determination of five to six elements is possible. The first results were very promising, since the measurements provided well defined, sharp, and well separated current peaks in the differential pulse mode [5,7]. Bismuth and its compounds are in general much less toxic to humans than other heavy metals [8]. This is explained by the low solubility of bismuth salts. Studies indicate that it does not bioaccumulate, or at least to a much lesser extent than other metals. Bismuth therefore seems to be a very promising and much more environmentally friendly alternative to mercury with comparable electrochemical properties. In the following years, more studies have been published concerning not only the voltammetric determination of zinc, cadmium, and lead [9,10], but also of other heavy metals such as nickel and cobalt [11–13]. The latter two species were measured by adsorptive stripping voltammetry (adSV), i.e., by complexation with dimethylglyoxime or nioxime and enrichment in the bismuth film under cathodic potentials, and subsequent stripping under more anodic potentials. However, the in situ deposition of the bismuth film under adsorptive stripping conditions turned out to be challenging. The adSV determination of nickel and cobalt is usually performed in an ammonia buffered solution, but bismuth suffers from hydrolysis in weakly alkaline media where insoluble bismuth hydroxide precipitates. To prevent precipitation, the bismuth film deposition was performed ex situ in an acetate buffered bismuth(II) solution. By using tartrate as stabilizing agent, Korolczuk et al. successfully managed the in situ bismuth film formation and adSV measurement [11].

Platinum metals are emitted into the environment by exhaust catalysts used nowadays in nearly every motorized vehicle [14,15]. With the increasing usage of polymer electrolyte membrane (PEM) electrolyzers and fuel cells with platinum as electrocatalyst, new possible sources for platinum emissions are evolving [16–20]. Exposure to platinum compounds may cause eyes, nose, or throat irritation as well as respiratory and skin allergies. Hence, environmental monitoring measures of platinum group metals are advisable. Moreover, since platinum group metals are quite expensive, recycling is of high importance.

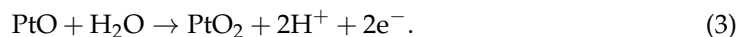
A further and increasingly relevant field of application for platinum analysis methods is the investigation of electrolyzer and fuel cell aging due to platinum dissolution. Platinum electrocatalysts typically used in low-temperature PEM fuel cells suffer from oxidation, which is accompanied by a reduction of electrochemically active surface area (ECSA) and finally by a loss of activity [17,21]. It has been reported that the cathode potential can locally increase up to 1.5 V, in particular during the start-up of the fuel cell with still insufficient gas supply [20]. A very recent X-ray photoelectron spectroscopy investigation has shown that at potentials above the platinum oxidation potential of approximately $1.0 V_{RHE}$, a Pt-PtO_x interface—also called 2D oxide, surface oxide, or oxide monolayer—is formed with contributions of both Pt²⁺ and Pt⁴⁺ species [22]. It has been speculated that the formed oxide layer is likely hydrous. A (surface) platinum(II) hydroxide could be formed by oxidation of platinum under humid conditions at high potentials:



Under dry conditions this hydroxide could be transformed into a (surface) platinum(II) oxide:



In addition, a subsequent oxidation to a (surface) platinum(IV) oxide is also comprehensible:

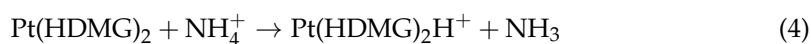


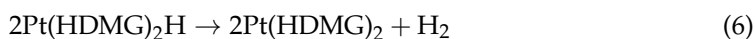
The thus formed platinum(II) or platinum(IV) ions can diffuse via the surface from the catalyst layer to the interface with the PEM of the fuel cell [23]. This effect causes a dissolution of the catalytically active platinum nanoparticles and hence a reduction of the ECSA, which severely limits the performance and lifetime of the entire fuel cell [24]. Moreover, molecular hydrogen from the anode crossing the membrane (“H₂ crossover”) can reduce Pt²⁺ or Pt⁴⁺ again to elemental platinum, which can subsequently redissipate or agglomerate to new but now wrongly placed platinum nanoparticles [20]. By this way, a characteristic “platinum band” is formed at the interface between catalyst-coated membrane and PEM. Moreover, platinum and platinum nanoparticles can migrate into the PEM, where it can catalyze severe deactivation reactions such as oxidation of water to hydroxyl radicals that can chemically destroy the membrane. Alternatively, not reduced platinum ions can dissolve in the product water and finally leave the fuel cell with the humid exhaust gas stream [16,25–28].

Therefore, online or mobile analysis of platinum in this product water during fuel cell operation can give direct insights into the current ageing state of a fuel cell and can help to make predictions of the end of its life. For all these reasons, sensitive, selective, and cost-efficient analytical methods are needed that ideally can be used in online measurements. Highly sensitive and selective, but also very expensive and bulky methods such as inductively coupled plasma - mass spectrometry (ICP-MS) are not useful for such applications. Instead, voltammetric methods can be considered as promising due to their rather low costs, compactness, and high sensitivities for many redox-active elements.

As for the determination of platinum group elements, the adSV method at a hanging mercury drop electrode (HMDE) exhibits superior limits of detection and quantitation in the low or even sub-nanogram per liter range [29,30]. The measuring principle of the detection of platinum at an HMDE is usually based on the formation of a platinum complex, which accumulates in the mercury electrode at cathodic potentials. Upon subsequent scanning to even more negative potentials, enriched platinum catalyzes the reduction of protons to molecular hydrogen by lowering mercury’s hydrogen overpotential. This resulting current flow is proportional to the amount of enriched platinum and its total concentration in the measurement solution. For platinum complexation, formaldehyde and hydrazine are added to the electrolyte forming a platinum(II) formazone complex following the reactions depicted in Figure 1 and according to Ref. [30].

As for the determination of platinum group metals, stripping voltammetry using the peak of the selective electrooxidation of lead from a lead-platinum-group metal electrolytic deposit on a graphite electrode has been tested as mercury electrode alternative [31,32]. Unfortunately, the heavy-metal lead is itself a toxic element, too. Alternatively, co-precipitation of platinum(IV) with copper or silver on graphite electrodes impregnated with polyethylene in combination with stripping voltammetry has been tested with limited success [33]. Bismuth films on glassy carbon exhibit a much more promising potential for the sensitive determination of platinum and rhodium with reported limits of detection in the ppt range [34,35]. Comparable to the HMDE, platinum can be determined on bismuth films by applying the adSV method. Usually, dimethylglyoxime (fully protonated form: H₂DMG; half-deprotonated form HDMG[−]) is used as complexing agent. In an ammonia buffer, the following reactions are reported to take place at the working electrode [34]:





Again, the current due to the formation of hydrogen is proportional to the concentration of accumulated platinum, which is proportional to its total concentration in the measurement solution.

The present publication deals with the validation of bismuth films deposited *ex situ* on glassy carbon solid state electrodes and on screen-printed glassy carbon electrodes for the determination of platinum in aqueous samples. The latter comprises for the first time a complete three-electrode on-chip approach that can be perfectly used in portable and online applications. The results are compared with the performance of an HMDE, and the methods were tested and discussed in terms of their applicability for the measurement of platinum in the product water of a real PEM fuel cell stack upon applying different load cycles.

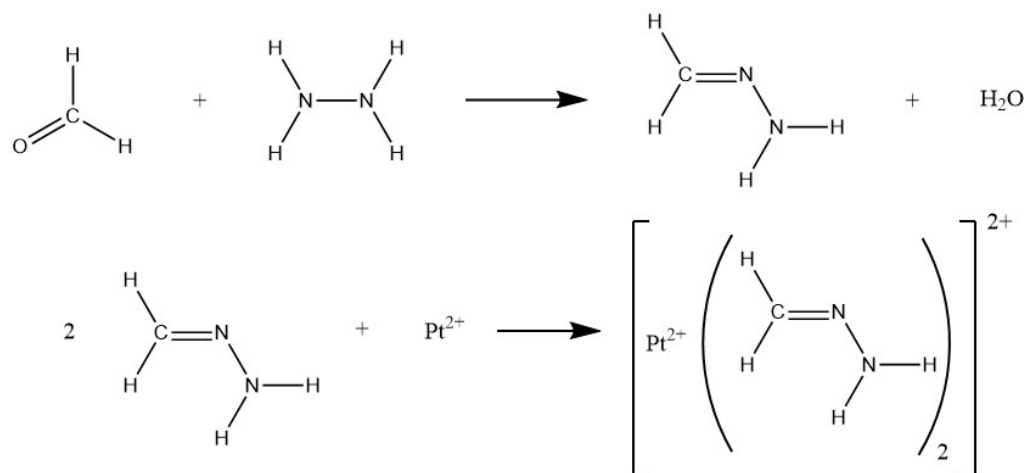


Figure 1. Reaction scheme explaining the adsorptive stripping voltammetric detection of platinum by HMDE with formaldehyde and hydrazine forming a platinum(II) formazone complex that is enriched in the mercury drop electrode under negative potentials.

2. Materials and Methods

2.1. Instrumentation

HMDE measurements were performed with a 797 VA Computrace voltammeter (Metrohm, Herisau, Switzerland), equipped with a multimode electrode filled with liquid mercury as working electrode, a glassy carbon electrode as auxiliary electrode, and an Ag/AgCl (3 M KCl) reference electrode.

As for measurements with a bismuth film electrode, a 663 VA Stand voltammeter (Metrohm, Herisau, Switzerland) connected to a PGSTAT204 potentiostat (Metrohm, Herisau, Switzerland) via the interface IME663 (Metrohm, Herisau, Switzerland) was used. The setup contained a three-electrode system consisting of an Ag/AgCl (3 M KCl) reference electrode, a glassy carbon auxiliary electrode, and a glassy carbon solid state electrode (GCE) as working electrode. The working electrode was coated with a bismuth film prior to Pt analysis, resulting in a bismuth film electrode (BiFE).

The 910 PSTAT mini setup (Metrohm, Herisau, Switzerland) was used for measurements with the bismuth film on screen-printed electrode (BiSPE). The electrode applied was a screen-printed DropSense electrode (Metrohm, Herisau, Switzerland) with a silver reference electrode, a carbon auxiliary electrode, and a 4 mm diameter glassy carbon working electrode on one chip.

All voltammetric measurements were performed in differential pulse adsorption stripping voltammetry (DPAdSV) mode and all given potentials were set against an Ag/AgCl (3 M KCl) reference electrode.

Continuous high load and dynamic load fuel cell tests were performed on a home-built fuel cell test station. The setup consisted of a commercial air-cooled, self-humidified,

open-cathode 100 W fuel cell stack (type H-100, Horizon Fuel Cell Technologies, Singapore) consisting of 20 individual fuel cells linearly connected by bipolar plates. Each cell was characterized by an anode catalyst loading of $0.08 \text{ mg/cm}^2 \text{ Pt/C}$, a cathode catalyst loading of $0.35 \text{ mg/cm}^2 \text{ Pt/C}$, and the $18 \text{ }\mu\text{m}$ thick GoreTM 18 polymer electrolyte membrane. The active area was about $20 \text{ cm}^2/\text{cell}$. The stack was operated with H_2 (5.0 purity grade, Westfalen, Münster, Germany) and ambient air. A digital pressure controller (Vögtlin Instruments, Muttenz, Switzerland) was used to hold a hydrogen overpressure of 0.5 bar at the inlet of the fuel cell stack and to assure a controlled hydrogen supply for every fuel cell load. A power supply (Voltcraft/Conrad Electronic, Hirschau, Germany) was used to run the air blower of the fuel cell. The power potentiostat PP211 and the electrochemical workstation Zennium Pro (both from ZAHNER-Elektrik, Kronach, Germany) were used to precisely program and potentiostatically control the respective load cycle applied to the fuel cell stack. A cold trap (glass flask in an ice bath) was connected with the exhaust gas outlet of the fuel cell to condense and collect the product water for platinum analysis. The fuel cell stack gas outlet was connected to a gas valve, which was automatically opened every 10 seconds to release the exhaust gas into the cold trap. Residual hydrogen in the exhaust gas was monitored by a hydrogen sensor (neo hydrogen sensors, Neuss, Germany).

2.2. Reagents

All chemicals used were of analytical grade purity (pro analysi) unless otherwise stated. 1000 mg/L bismuth and platinum stock solutions were purchased from CPI international (Santa Rosa, USA) and Merck (Darmstadt, Germany), respectively, and diluted as required. For the preparation of the Pt standard solutions, the appropriate amount of Pt stock solution was dissolved in 0.1 M hydrochloric acid (32%, Bernd Kraft, Duisburg, Germany). To prepare the coating solution, 100 mg/L bismuth solution was added to a 0.2 M 1:1 sodium acetate (>99%, Merck, Darmstadt, Germany)/acetic acid (>99%, Carl Roth, Karlsruhe, Germany) buffer. Ammonia (25%, Carl Roth, Karlsruhe, Germany)/ammonium chloride (99.5%, reinst Ph. Eur., Grüssing, Filsum, Germany) buffer containing $5 \times 10^{-5} \text{ mol/L}$ dimethylglyoxime (DMG; >99%, Fluka, Seelze, Germany) served as electrolyte for the BiFE measurement. A 0.1 M DMG stock solution was prepared by dissolving the appropriate amount of DMG in pure ethanol.

For HMDE measurements, a solution of 0.72 mol/L sulfuric acid (95–97%, Bernd Kraft, Duisburg, Germany), 3 mmol/L hydrazine sulfate (>99%, Fluka, Seelze, Germany) and 6.71 mmol/L formaldehyde (37%, AppliChem, Darmstadt, Germany) served as electrolyte. The electrolyte solution had to be prepared every day due to its instability.

All solutions were prepared from Milli-Q water.

2.3. BiFE and BiSPE Preparation

The following procedure was used for coating the solid state electrode and the screen-printed electrode. The coating solution consisted of a 0.2 M sodium acetate/acetic acid buffer containing 100 mg/L bismuth. The working electrode was cleaned with Milli-Q water and then immersed in the coating solution. Before coating, 50 cleaning cycles were performed on the solid state electrode in the range of -0.6 to -1.1 V . On the screen-printed electrode no cleaning steps were applied since this option is missing for the used 910 PSTAT mini setup. For both electrodes, a cleaning potential of -0.15 V was applied for 2 s.

For the accumulation mode, a potential of -1.0 V was applied for 300 s. During coating, the solution was stirred at 200 rpm. After a rest time of 5 s, a voltammogram was recorded in the range of -0.6 and -1.1 V with a sweep rate of 0.04 V/s , a pulse amplitude of 0.05 V , and a pulse time of 0.04 s . After coating, the electrode was carefully rinsed with Milli-Q water.

2.4. Procedure for Pt Determination at the BiFE and BiSPE

Except for the cleaning and purging step, the same procedure was used for both the solid state and screen-printed electrode. On the screen-printed electrode there was

no possibility for a purging and cleaning step before the measurement with the used 910 PSTAT mini setup. For the determination of platinum, 9 mL of electrolyte consisting of a 0.01 M ammonia/ammonium chloride buffer (pH = 9.25) containing 5×10^{-5} mol/L DMG was used. 1 mL of sample was added to the electrolyte. The platinum solutions used consisted of the appropriate amount of a 1 g/L platinum standard solution dissolved in 0.1 M hydrochloric acid. Electrolyte as well as platinum solutions had to be prepared daily due to their instability. Prior to each measurement, the measurement solution was purged with N₂ (4.8, Westfalen, Münster, Germany) for 300 s to eliminate O₂ in the solution of the solid state electrode. In addition, cleaning cycles were performed before analysis at this electrode. For this, a potential between -0.4 and -1.4 V was cycled for 50 times. At both electrodes an accumulation potential of -0.7 V was applied for 60 s while the solution was stirred at 200 rpm. After 10 s of equilibration time, the voltammogram was recorded from -0.4 to -1.4 V with a sweep rate of 0.04 V/s in differential pulse mode. The pulse amplitude was set to 0.05 V and the pulse time was 0.04 s. For all measurements, the measuring cell was cooled in an ice bath.

2.5. Procedure for Pt Determination at the HMDE

Pt determination at the HMDE was carried out in 1.5 mL electrolyte consisting of 0.72 mol/L sulfuric acid, 3 mmol/L hydrazine sulfate, and 6.71 mmol/L formaldehyde. The electrolyte was added to 10 mL of the sample. Before the measurement, the measuring cell was purged with N₂ (4.8, Westfalen, Münster, Germany) for 300 s to remove O₂. An accumulation potential of -0.6 V was then applied for 120 s while the solution was stirred at 2000 rpm. After an equilibration time of 10 s, a scan from -0.6 to -1.1 V was performed in differential pulse mode. The sweep rate was set to 0.02 V/s and the pulse amplitude was 0.05 V.

2.6. Sample Preparation

The condensed fuel cell product water was stored in polypropylene sample vessels at -18 °C after collection. To ensure stability, 0.01 mL concentrated hydrochloric acid was added per 10 mL sample. The sample vessels were cleaned with 10% HNO₃ (65%, Bernd Kraft, Duisburg, Germany) and Milli-Q water before use.

Prior to each analysis, samples were treated with UV irradiation in a 909 UV Digester (Metrohm, Herisau, Switzerland). To each 10 mL sample, 0.01 mL concentrated hydrochloric acid and 0.05 mL hydrogen peroxide solution (30%, Carl Roth, Karlsruhe, Germany) were added. The UV treatment of the prepared samples was run for 90 min at 90 °C.

2.7. Procedure for Continuous High Load and Dynamic Load Fuel Cell Tests

Two different load profiles were used for the fuel cell test studies. The continuous high load cycle was run at constantly high power at approximately 100 W by potentiostatically holding the fuel cell stack voltage at 13 V. The dynamic cycle was adapted from the worldwide harmonized light duty vehicle test procedure (WLTP) [36]. To generate as much product water as possible, only the most power intensive sections “high” and “extra high” of the WLTP were used. To create the program code, speed values of the WLTP were first linearly converted into percentages, i.e., 100% corresponded to maximum speed. The percentages obtained were then transferred to the set power of the fuel cell with 100% corresponding to maximum power. For this purpose, a polarization curve was recorded for the fuel cell stack on the test station to obtain the corresponding voltage for each power setting. With the obtained voltages a dynamic test cycle was programmed and applied to the fuel cell stack (potentiostatic control with potentiostat/electrochemical workstation).

3. Results

3.1. Validation of the HMDE

First of all, the HMDE was validated for the determination of platinum in aqueous samples. An image of the HMDE measuring cell is depicted in Figure 2a. To identify

the working range, voltammograms were recorded in the concentration range between 5.0 and 40.0 ng/L platinum (Figure 3a). The resulting averaged peak currents were then plotted against the respective platinum concentration in order to obtain the calibration curve (Figure 3b). For the linear regression a determination coefficient R^2 of 0.9997 was calculated. In order to prove the linearity, the point-to-point gradient was determined and compared with its median. As can be seen in Figure 3c, only little (<10%) and no systematic deviation from the median is observed. Accordingly, the platinum measurement in the range of 5.0–40.0 ng/L is to be assumed as linear and this range can be defined as working range. We also checked the working range of 50.0–400.0 ng/L platinum. However, the point-to-point deviation resulted in a large (>10%) and systematic deviation from the median above concentrations of 250 ng/L. This shows that the meaningful use of the method should be limited to lower concentrations.

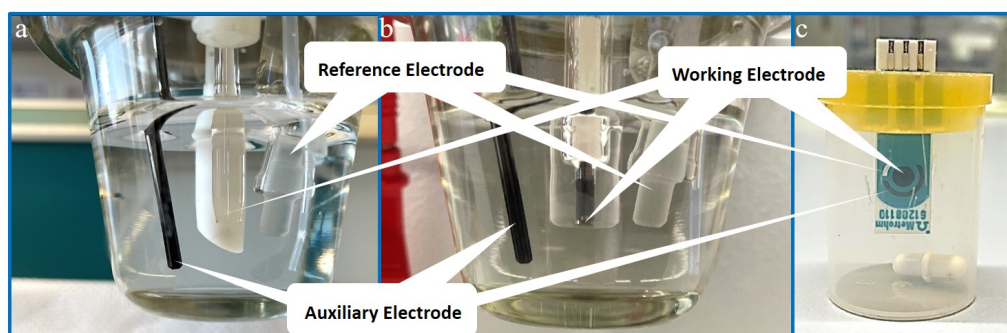


Figure 2. Photographs of the used voltammetric measurement cells: (a) HMDE setup, (b) solid state electrode setup for BiFE measurement, (c) measuring cell with screen-printed electrode for BiSPE measurement.

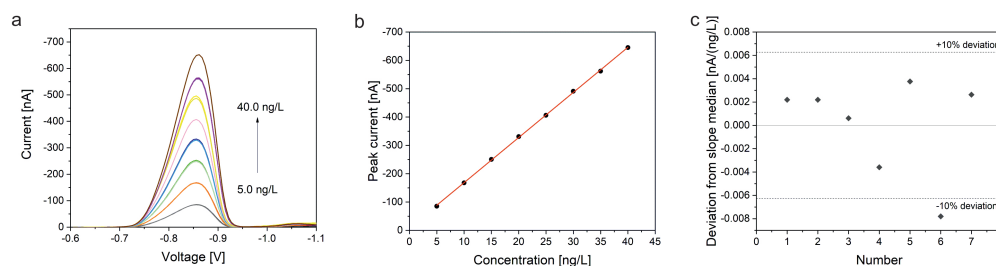


Figure 3. (a) Recorded HMDE voltammograms of different platinum standard solutions. (b) Resulting calibration curve with linear regression (red line) (after subtraction of blank values). (c) Results of the point-to-point gradient linearity test of the linear calibration curve.

Limits of detection (LOD) and quantification (LOQ) were calculated after DIN 32645 by using the 5.0–40.0 ng/L calibration line. For the LOD a value of 0.76 ng/L and for the LOQ a value of 2.75 ng/L was obtained (with type I error α of 0.05 and result uncertainty $1/k$ with $k = 3$). The LOQ was successfully verified with a measurement of a sample containing 2.8 ng/L platinum. These limits are in good agreement with results published by other groups measured under comparable conditions [14,15,37,38].

In order to prove the accuracy of the method, three samples of tap water were each spiked with 10.0 ng/L platinum. These samples were first treated with UV irradiation prior to the measurement to eliminate organic interfering substances. Afterwards, the platinum content was measured by standard addition and recovery rates were calculated. The obtained values are summarized in Table 1. As a result, an average recovery rate of 106.8% was obtained.

Table 1. Determined platinum concentrations and recovery rates for three independent tap water samples each spiked with 10.0 ng/L platinum as measured by HMDE.

Sample	Concentration in ng/L	Recovery Rate in %
Sample 1	12.10	121.0
Sample 2	10.82	108.0
Sample 3	9.12	91.2

For the determination of the precision and repeatability of the method, respectively, three Milli-Q water samples were each spiked with 10.0 ng/L platinum. The concentration of platinum of the samples was determined by standard addition. This procedure was repeated analogously on a second day with three newly prepared samples. All results are summarized in Table 2. As a result, the relative standard deviation (RSD) was 4.6% on the first day, 10.0% on the second day, and 8.4% over all measurements. However, on the second day one sample could be identified as statistical outlier. If this one is removed, an overall RSD of 4.2% is received.

Table 2. Mean values, standard deviations, and relative standard deviations (RSD) as calculated from the voltammetric investigation of six independent Milli-Q water samples (three per day) each spiked with 10.0 ng/L platinum as measured by HMDE.

Measurement Day	Mean Value in ng/L	Standard Deviation in ng/L	RSD in %
Day 1	10.2	0.5	4.6
Day 2	11.0	1.1	10.0
Average over all days	10.6	0.9	8.4

3.2. Validation of Bismuth Film on Solid State Glassy Carbon Electrode

An image of the BiFE measuring cell is depicted in Figure 2b. To validate the bismuth film electrode, several preliminary tests had been made to find optimal parameters regarding electrolyte composition, rotational speed during film deposition, bismuth concentration, oxygen content of the measurement solution, sample volume, and platinum concentration. As a result, the sensitivity of the method increased with nitrogen purging to remove dissolved oxygen. Moreover, best results were obtained with a very slow rotational speed of only 200 rpm during film deposition and platinum enrichment. Despite all of these improvements, we could not confirm the detection of platinum in the ppt range as was claimed by Ref. [34] for a comparable setting. Moreover, we could not find any other independent source confirming these surprisingly high sensitivities for platinum on bismuth films. In our experiments, a reproducible calibration with clearly identifiable peaks associated with platinum was only possible within the working range of 50.0–400.0 µg/L platinum in the sample (Figure 4a). The calibration curve with eight measurement points in this range is depicted in Figure 4b. Linearity could be proven by the high determination coefficient R^2 of 0.9994. Additionally, the results of the point-to-point gradient exhibit little (<10%) deviations from the slope median (Figure 4c). There seems to be a trend with higher deviations from the slope median towards higher concentrations, but the variations within the checked working range are still below the 10% threshold. LOD and LOQ values were determined from this linear calibration after DIN 32645. As a result, an LOD of 7.93 µg/L and an LOQ of 29.1 µg/L was determined (with type I error α of 0.05 and result uncertainty $1/k$ with $k = 3$).

The accuracy of the method was checked by measuring the recovery rate with three tap water samples each spiked with 100.0 µg/L platinum. The results are summarized in Table 3. All samples were first pretreated by UV irradiation. Afterwards, the platinum concentration was determined by standard addition. The measurements resulted in an average recovery rate of 113.6%.

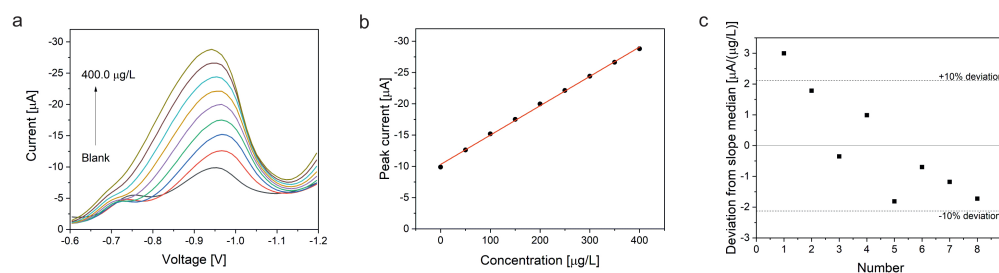


Figure 4. (a) Recorded voltammograms of different platinum standard solutions as measured on a bismuth film on solid state glassy carbon electrode. (b) Resulting calibration curve with linear regression (red line). (c) Results of the point-to-point gradient linearity test of the linear calibration curve.

Table 3. Determined platinum concentrations and recovery rates for three independent tap water samples each spiked with 100.0 µg/L platinum as measured with a bismuth film on solid state glassy carbon electrode.

Sample	Concentration in µg/L	Recovery Rate in %
Sample 1	109.3	109.3
Sample 2	123.4	123.4
Sample 3	108.0	108.0

Finally, the precision of the method using a bismuth film electrode was validated by preparing three Milli-Q water samples each spiked with 100.0 µg/L platinum. The platinum content of the three samples was determined by standard addition. The procedure was repeated on a second day with three newly prepared samples. Obtained mean values, standard deviations, and RSD values are summarized in Table 4. We obtained an RSD of 6.5% for the first day, of 5.4% for the second day, and of 5.9% for all six samples.

Table 4. Mean values, standard deviations, and relative standard deviations (RSD) as calculated from the voltammetric investigation of six independent Milli-Q water test samples (three per day) each spiked with 100.0 µg/L platinum as measured with a bismuth film on solid state glassy carbon electrode.

Measurement Day	Mean Value in µg/L	Standard Deviation in µg/L	RSD in %
Day 1	102.4	6.6	6.5
Day 2	107.4	5.8	5.4
Average over all days	104.9	6.2	5.9

3.3. Validation of Bismuth Film on Screen-Printed Electrode

The determination of platinum at a bismuth film deposited on a glassy carbon solid state and screen-printed electrode, respectively, was carried out after very similar protocols. Only the parameters set on the potentiostat were adjusted. An image of the BiSPE measuring cell is depicted in Figure 2c. This is to the best of our knowledge the first time that platinum was determined by using the full functionality of a screen-printed (all on-chip) electrode with a deposited bismuth film on screen-printed glassy carbon as working electrode, screen-printed glassy carbon as counter electrode, and screen-printed silver as reference electrode. In all other known studies with bismuth films on screen-printed electrodes, the screen-printed working electrode was contacted to a conventional solid state counter and reference electrode in a conventional (bulky) three-electrode cell setup.

To determine the working range and the LOD and LOQ values of the BiSPE, a calibration line was first recorded. For this purpose, 10 calibration points in the range of 50.0–500.0 µg/L were measured. Concentrations above 500 µg/L could not be analyzed because a saturation effect was detected there. At concentrations below 50 µg/L, no signal

associated with platinum could be identified. The resulting voltammograms are shown in Figure 5a and the corresponding calibration diagram is depicted in Figure 5b. The visual consideration of the calibration points and the rather low coefficient of determination R^2 of 0.981 suggests that there is no linearity. To check this assumption, a linearity test was performed. For this purpose, the deviations from the slope median were calculated and plotted in a diagram (Figure 5c). A trend can be clearly seen in the linearity test with significant deviations from the 10% threshold at both low and high concentrations. Therefore, the concentration range of 50–500 $\mu\text{g/L}$ is to be considered as non-linear. For this reason, a regression with a 2nd order polynomial calibration function was run (Figure 5b). It can be seen visually and from the coefficient of determination ($R^2 = 0.9993$) that a 2nd order regression shows a much better correlation than the linear calibration. To further illustrate this, the residuals were also calculated and plotted for both regression functions (Figure 5d). When comparing the residuals of the 1st and 2nd order polynomial, it can be clearly seen that the residuals are significantly smaller for the 2nd order calibration function.

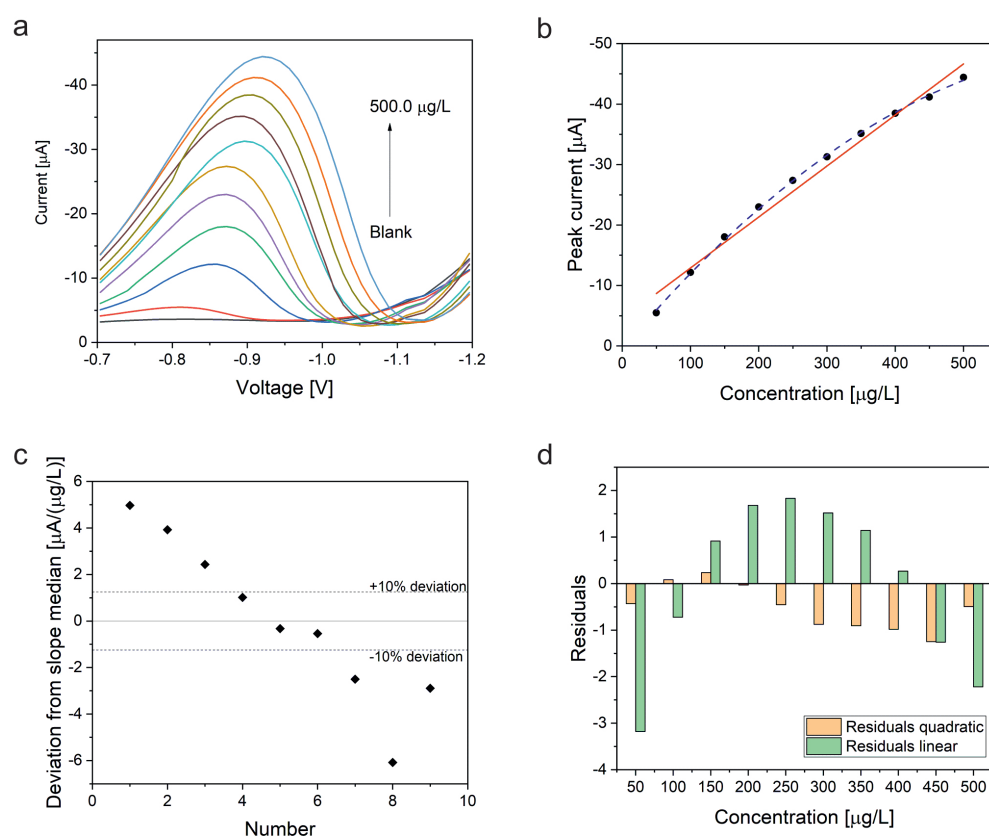


Figure 5. (a) Recorded voltammograms of different platinum standard solutions as measured on a bismuth film on screen-printed glassy carbon electrode. (b) Resulting calibration curve with linear (red solid line) and quadratic (blue dashed line) regression. (c) Results of the point-to-point gradient linearity test for the first order regression curve. (d) Plot of the residuals of the linear and quadratic regression, respectively.

The calibration curve method after DIN 32645 adapted to a 2nd order calibration function was applied to determine the LOD and LOQ values. As a result, an LOD of 22.5 $\mu\text{g/L}$ platinum and an LOQ of 79.0 $\mu\text{g/L}$ platinum was calculated (with type I error α of 0.05 and result uncertainty $1/k$ with $k = 3$). For comparison, LOD and LOQ values were also calculated with the linear regression curve. Here, an LOD of 45.9 $\mu\text{g/L}$ and a LOQ of 151 $\mu\text{g/L}$ was obtained.

The precision of this method was determined at a concentration of 250 $\mu\text{g/L}$ platinum. Due to the observed saturation effect of this method, the working range was limited to a

maximum platinum concentration of 500 $\mu\text{g/L}$. Therefore, no meaningful standard addition in equidistant steps was possible for a concentration of 250 $\mu\text{g/L}$. For this reason, Milli-Q water was first spiked with 200.0 $\mu\text{g/L}$ platinum and defined as “blank”. Then, 50.0 $\mu\text{g/L}$ platinum was added. This was defined as sample. This concentration was chosen because it ensured that the platinum concentration was safely above the LOQ after both linear and quadratic regression. Finally, the concentration of this added platinum amount was determined by standard addition. The experiment was repeated for three independent samples on one day and three additional samples on a second day. The concentrations were calculated with both 1st and 2nd order calibration functions. From this, recovery rates were calculated. The results are listed in Table 5.

Table 5. Determined platinum concentrations and recovery rates for test samples containing 50.0 $\mu\text{g/L}$ platinum (in a 200.0 $\mu\text{g/L}$ platinum “blank”, see text above) measured with a bismuth film on screen-printed electrode.

Day/Sample	Concentration in $\mu\text{g/L}$ (1st Order Calibration)	Recovery Rate in % (1st Order Calibration)	Concentration in $\mu\text{g/L}$ (2nd Order Calibration)	Recovery Rate in % (2nd Order Calibration)
Day 1/Sample 1	71.4	143	51.7	103
Day 1/Sample 2	62.6	125	54.0	108
Day 1/Sample 3	60.4	121	50.6	101
Day 2/Sample 1	62.6	126	50.6	101
Day 2/Sample 2	63.8	128	53.6	107
Day 2/Sample 3	64.1	128	51.3	103

From the measured values, mean value, standard deviation, and RSD were determined. The data are summarized in Table 6. It can be seen from the table that the standard deviation for the 1st order calibration take a total value of 3.8 $\mu\text{g/L}$. The standard deviation over all days for the 2nd order calibration has a value of 1.5 $\mu\text{g/L}$. When considering the RSD, it is always below 10%. When only applying the 2nd order calibration function, the RSD is even always below 5%. Both standard deviation and RSD allow the assumption that a very good precision can be achieved by using the quadratic calibration function. In addition, the recovery rates measured with the 2nd order polynomial are with 104% on average for all days significantly better than the values measured with the linear calibration function (average for all days: 129%). These results confirm the earlier assumption that the 2nd order polynomial calibration is superior to the linear calibration.

Table 6. Mean values, standard deviations, and relative standard deviations (RSD) as calculated from the voltammetric investigation of test samples containing 50.0 $\mu\text{g/L}$ platinum measured with a bismuth film on screen-printed electrode.

Measurement Day	Mean Value in $\mu\text{g/L}$ (1st Order Calibration)	Mean Value in $\mu\text{g/L}$ (2nd Order Calibration)	Standard Deviation in $\mu\text{g/L}$ (1st Order Calibration)	Standard Deviation in $\mu\text{g/L}$ (2nd Order Calibration)	RSD in % (1st Order Calibration)	RSD in % (2nd Order Calibration)
Day 1	64.8	52.1	5.8	1.7	9.0	3.3
Day 2	63.6	51.9	0.65	1.5	1.0	3.0
Average over all days	64.2	52.0	3.8	1.5	5.9	2.8

3.4. Determination of Platinum in the Product Water of a PEM Fuel Cell

Two different load profiles were applied to a 100 W PEM fuel cell stack to obtain product water as realistic test sample for the voltammetric ultratrace determination of platinum. An image of the fuel cell test setup is depicted in Figure 6.

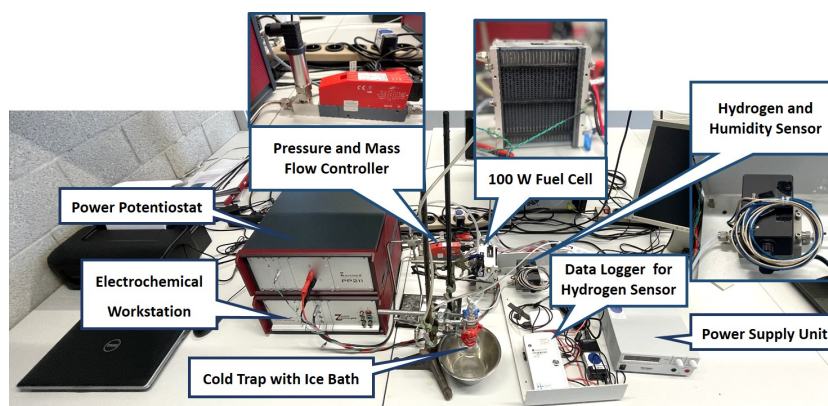


Figure 6. Photograph of the used fuel cell stack test setup.

The different load profiles were applied to reflect different stress scenarios: continuous high power at about 100 W and dynamically alternating power between minimum and maximum power. The dynamic cycle was adapted from the worldwide harmonized light duty test procedure (WLTP). This protocol was developed by the United Nations Economic Commission for Europe (UNECE) and serves the purpose of determining the pollutant emissions of passenger cars and light commercial vehicles [36]. Depending on the performance of the vehicle, a distinction is made between three different classes. Passenger cars are classified in class 3. This test cycle is divided into four parts according to maximum speed: low, medium, high, and extra high speed. In order to produce as much product water as possible, only the most power-intensive sections “high” and “extra high” were used for the dynamic stress test in this work. The resulting potential, current, and power curves are depicted in Figure 7a. The profile shown corresponds to one loop, which is repeated a total of 14 times. This results in a total cycle time of approximately 6 hours. For operation at continuous high load, a voltage of 13 V was applied for approximately 6 hours. This corresponds to a current of approximately 8 A and a power of approximately 105 W (Figure 7b).

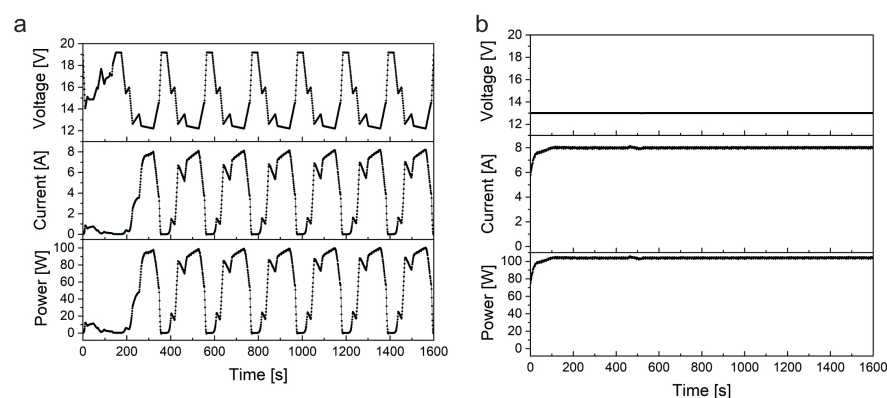


Figure 7. (a) Dynamic load cycle as adapted from the “high” and “extra high” sections of the WLTP test cycle. The depicted loop was repeated for 14 times and applied to a 100 W fuel cell stack. (b) First part of the continuous high load cycle applied to a 100 W fuel cell stack. The high load was applied for approximately 6 hours. Note that in both test schemes the voltage was set by the electrochemical workstation/potentiostat (i.e., potentiostatic control), while the corresponding current was measured. The power was calculated from both values.

During load cycling, more parameters such as the applied hydrogen pressure and flow rate as well as the measured stack temperature were logged. In addition, polarization curves were recorded before and after the stress tests. A representative set of data is shown in Figure 8.

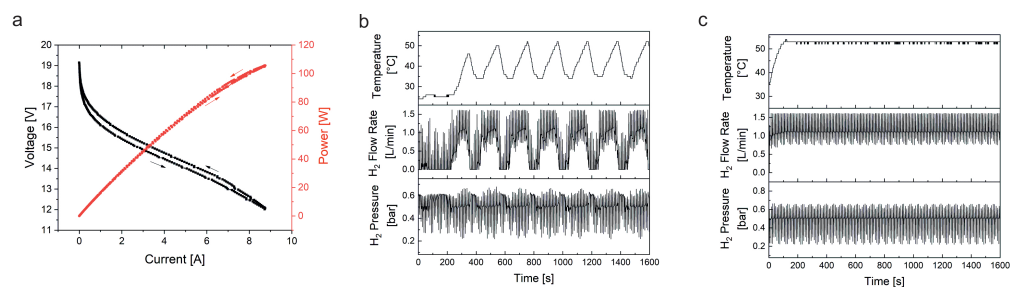


Figure 8. (a) Representative polarization curve of the investigated fuel cell stack. (b) Typical pressure, flow rate, and fuel cell stack temperature chart recorded during the dynamic load cycle. (c) Respective chart for the high load cycle. Please note that the observed spikes in the pressure and flow rate charts are due to the exhaust gas valve which is automatically opened every 10 seconds.

Moreover, the produced water was continuously collected from the PEM fuel cell during the different load cycle protocols and investigated by voltammetry. We started with measurements at the HMDE due to its lowest LOQ and since we expected very low platinum concentrations. Since the expected concentration range of platinum in the product water was completely uncertain, a calibration line in the range of 10–60 ng/L was first recorded. Thus, when the fuel cell sample was first measured, the approximate concentration could be estimated. It turned out that the concentrations of the samples are so low that they can only be measured by the HMDE, but not by the bismuth film electrodes. The exact platinum concentration in the fuel cell product water was hence measured by standard addition calibration with the HMDE. The results of the dynamic cycle measurement are shown in Figure 9. Platinum could be successfully determined as can be seen from the well-developed peaks with a maximum at approximately -0.88 V. The peak voltages corresponding to the platinum standard additions match nearly perfectly with the original peak of the sample. The determined platinum concentration in this sample was (2.93 ± 0.11) ng/L. The result was confirmed by measuring a second sample. The obtained platinum concentration of this second sample was (3.17 ± 0.20) ng/L, resulting in an average amount of 3.1 ng/L Pt for the product water obtained during the dynamic test cycle. If the amount of platinum in the entire sample is related to the fuel cell runtime in which the product water was obtained, an average of 0.54 pg/h or 8.3×10^{-19} g/(cm²s) platinum is lost (related to the active geometric surface area of the fuel cell stack consisting of 20 single cells with an individual geometric area of 20 cm²). It is further to be mentioned that an additional signal peaking at -0.98 V appeared in the sample's voltammogram which barely changed with the standard additions.

Next, the sample from the fuel cell was measured which was run in the high load profile. The results are shown in Figure 10. Here, a platinum concentration of (4.02 ± 0.05) ng/L was determined. This measurement was checked by a second sample, too. In this case, a platinum concentration of (4.09 ± 0.05) ng/L was obtained, resulting in an average platinum concentration of 4.1 ng/L. Consequently, a platinum dissolution of 2.2 pg/h or 3.3×10^{-18} g/(cm²s) can be calculated. As in the voltammogram of the dynamic cycle, a second signal peaking at -0.98 V can be seen here as well.

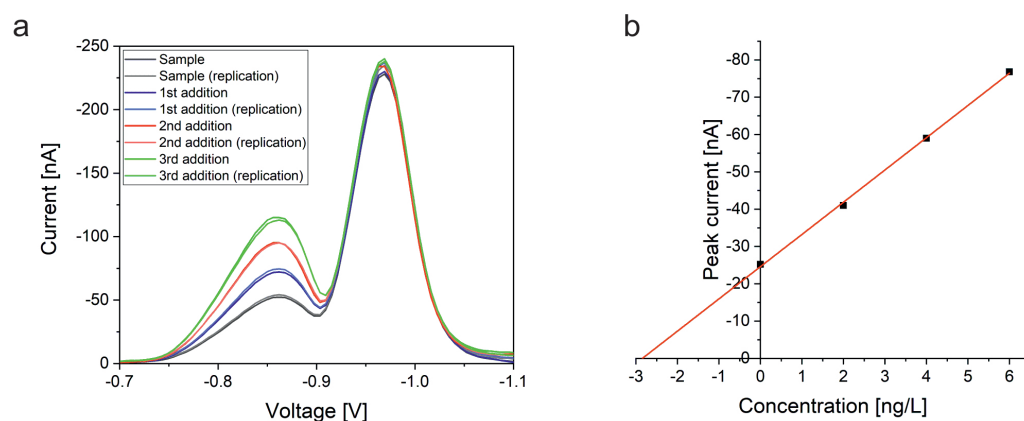


Figure 9. (a) Recorded voltammograms of fuel cell product water collected during the dynamic load cycle and the corresponding results of the standard addition calibration as measured by HMDE. (b) Resulting calibration curve with linear regression (red line) after background subtraction.

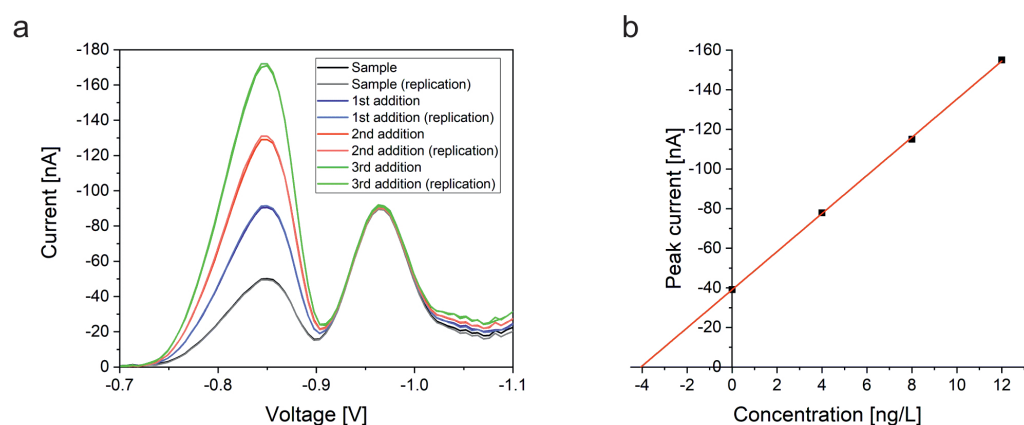


Figure 10. (a) Recorded voltammograms of fuel cell product water collected during the continuous high load cycle and the corresponding results of the standard addition calibration as measured by HMDE. (b) Resulting calibration curve with linear regression (red line) after background subtraction.

4. Discussion

Our presented work focuses on methods for the determination of platinum using the HMDE and bismuth film electrodes deposited on glassy carbon. Platinum determination by adsorptive stripping voltammetry with an HMDE is a standard method and the method could be successfully validated for the quantitation of platinum in the product water of a 100 W fuel cell stack. As for the bismuth film on glassy carbon solid state electrode, various conditions were optimized. After a successful development of the method, it was also successfully validated for the determination of platinum by adSV. During the validation it turned out that both methods produce reproducible results with high accuracy. In addition, linear working ranges could be defined. Detection and determination limits were determined using the calibration line method. LOD and LOQ values of the method based on the HMDE are in a concentration range more than three orders of magnitude lower than those obtained with the bismuth film electrode.

In the validation of the bismuth film on a screen-printed glassy carbon electrode, no clear linear relationship between concentration and current was found. A much better fit was obtained by using a second-order calibration function. One factor that could affect linearity is the nature of the bismuth film. The bismuth film could not have formed ideally or may have become unstable, resulting in a detachment from the carbon electrode as a consequence of repeated adsorption and desorption of the analyte. Another reason could

be the change in the morphology of the bismuth film during the measurements as reported by Baldrianova et al. [39]. It should be noted that no conditioning cycles were carried out prior to the measurement in order to clean the electrode. So there could be impurities on the electrode surface that occupy the adsorption sites. Furthermore, no conventional Ag/AgCl electrode was used as the reference electrode, but a screen-printed silver electrode. Unlike the Ag/AgCl electrode, this electrode is in direct contact with the measurement solution. It is therefore possible that the reference electrode potential changes during the measurement and could influence the voltage setting. Moreover, no nitrogen purging was performed prior to the measurement. Hence, the dissolved oxygen or its reduction products such as hydrogen peroxide could also negatively affect the stability of the film or the adsorption reaction of the platinum complex. Van der Linden et al. showed that the presence of oxygen in the solution prevents the formation of monolayers on mercury films [40]. A similar behavior is also thinkable for bismuth films. In general, all effects that result in passivation of the electrode could be a reason for the non-linear behavior. In this case, fewer and fewer active centers would be available for adsorption of the analyte complex, which leads to ever smaller signals. However, the validation with the quadratic calibration function gave a very good precision and recovery rate proving the principle applicability of this method for the determination of platinum. Overall, the accuracy of all three methods is with average recovery rates of 106.8% (HMDE), 113.6% (BiFE), and 103.8% (BiSPE) very good. In addition, a high precision could be proven for all methods as well, as supported by average RSD values of 4.2% (HMDE; without outlier), 5.9% (BiFE), and 2.8% (BiSPE), respectively, obtained by analyzing six standard samples measured at two different days.

Due to the rather high LOD and LOQ values of the bismuth film electrodes, only the HMDE could be used to measure the platinum dissolution in fuel cells. In the product water of the measured 100 W fuel cell stack, a signal at -0.88 V showed up that can be unambiguously assigned to platinum. As a result, platinum dissolution rates of 8.3×10^{-19} g/(cm²s) for the dynamic cycle and 3.3×10^{-18} g/(cm²s) for the continuous high load cycle were measured. Obviously, the effect of a constantly high current density (and low voltage) results in an approximately four times higher platinum dissolution rate than observed in the dynamic cycle. Usually, stronger platinum oxidation is observed at higher potentials (close to the open circuit potential, OCP) and the membrane is mechanically more stressed under dynamic potential cycling conditions. However, since with the higher current in the constant high load cycle more product water is generated per time, it might cause a stronger leaching out of soluble platinum. The dissolution rates found in our study are still orders of magnitude lower than the ones reported by Wang et al. ($1.4\text{--}1.7 \times 10^{-14}$ g/(cm²s)) [16]. In contrast to our measurements, they measured the platinum dissolution of carbon supported platinum nanoparticles at a potential of 0.9 V, which is close to the OCP. At this potential, platinum is much more likely to be oxidized which might explain the higher platinum dissolution. Xie et al. do not give a concrete dissolution rate, but report on a platinum concentration of 40–160 ppt in the cathodic product water of a fuel cell aged in a cyclic voltammetry measurement under high-humidity conditions for up to 2000 h [27]. These values are only slightly higher than the concentrations observed in our experiment.

In addition to the platinum peak, a second peak at -0.98 V appeared in the voltammogram of the fuel cell product water. The peaks are sufficiently separated, hence the platinum analysis was fortunately not disturbed. A literature search revealed that with formazone also rhodium can be analyzed [14]. The peak potential of rhodium is expected at approximately -1.1 V. This, however, does not agree very well with the peak found at -0.98 V in our case. Palladium is another platinum group element which is often found in conjunction with platinum and rhodium in catalytic applications. However, the expected palladium signal at -0.7 V [14] does not match well with the signal in question. However, it has been reported that zinc can interfere with platinum when using formazone as complexing agent. A peak at approximately -1 V was associated with such zinc species [29,41]. For this reason it seems plausible that the additional peak might be caused by zinc. For an

accurate and reliable identification of the second peak further experiments are essential, but were not the focus of this study.

5. Conclusions

The aim of our work was to validate different voltammetric methods to determine the platinum concentration in the product water of a hydrogen PEM fuel cell. The investigated fuel cell stack was run under two different load cycles: a dynamic cycle with dynamically changing the load between low and high power and a continuous high load profile. As for the voltammetric methods, a classic HMDE was compared with a bismuth film on glassy carbon solid state electrode and a bismuth film on a screen-printed electrode (with all electrodes including counter and reference electrode on one chip). With all methods highly reproducible and precise results were obtained. However, LODs and LOQs differed significantly. The best values were obtained for the HMDE with an LOD of 0.76 ng/L and an LOQ of 2.8 ng/L. The bismuth film electrodes exhibited much higher values. The bismuth film on solid state glassy carbon showed an LOD of 7.9 µg/L and an LOQ of 29.1 µg/L, whereas with the bismuth film on screen-printed glassy carbon an LOD of 22.5 µg/L and an LOQ of 79.0 µg was measured after applying a quadratic calibration function. Obviously, the LODs of bismuth films in the ppt range for platinum as reported before [34,35] could not even closely be reproduced. Reasons are hard to be identified since no analytically satisfying validation of the method was presented in the previously published results. This let us come to the conclusion that bismuth films are still no alternative for replacing the HMDE in the ultratrace determination of platinum (i.e., ppt range), but that they are capable for trace analysis in the ppb range. We could also prove for the first time that a compact, rather cheap, and disposable on-chip sensor with a bismuth film as working electrode can be used for voltammetric online or “one-shot” decentralized platinum trace analysis. The HMDE method bears the severe disadvantages that it needs a special designed multimode electrode for the reproducible and stable formation of mercury drops and that it consumes toxic liquid mercury, which has to be disposed of as special hazardous waste. This makes this method much more expensive than simpler voltammetry settings. In contrast, bismuth film electrodes consume only very small amounts of non-toxic bismuth salt solutions, which can even be reused for several times. The setup for the screen-printed electrode with the portable potentiostat is even less expensive than a standard voltammetry stand with conventional solid state electrodes. The screen-printed electrode can be reused, but it can also be used as disposable item to avoid cross contamination from former analyses.

However, in our application only the HMDE proved to be useful for the determination of platinum in the product water of a 100 W PEM fuel cell stack. The stress tests based on the dynamic load profile resulted in a loss of 0.54 pg/h platinum. As for the continuous high load test, an even higher platinum loss of 2.2 pg/h was observed. This gives principal evidence that the fuel cell deactivation can be monitored by voltammetric methods in terms of a sensitive detection of dissolved platinum in the product water. In the future, the fabrication of bismuth films or of other alternatives on screen-printed electrodes has to be better understood and to be improved in order to develop powerful sensors that can be successfully applied in online and mobile measurements with ultratrace sensitivity.

Author Contributions: Conceptualization, M.E.; methodology, M.E.; software, L.B.; validation, L.B. and M.E.; formal analysis, L.B. and M.E.; investigation, L.B.; resources, M.E.; data curation, L.B. and M.E.; writing—original draft preparation, L.B. and M.E.; writing—review and editing, M.E.; visualization, L.B. and M.E.; supervision, M.E.; project administration, M.E. All authors have read and agreed to the published version of the manuscript.

Funding: Funding of the project “Intelligent Fuel Cell” by LEONARDO—Center for Creativity and Innovation and the initiative “Innovative Hochschule” of the Federal Ministry for Education and Research is gratefully acknowledged.

Institutional Review Board Statement: Not applicable.

Informed Consent Statement: Not applicable.

Data Availability Statement: Not applicable.

Acknowledgments: The authors thank Marco Lindner for preliminary experiments and Isabel Wittman and Susanne Thiel for laboratory support. Steven Schamber is gratefully acknowledged for his assistance in installing the fuel cell test stand.

Conflicts of Interest: The authors declare no conflict of interest.

References

1. Zuman, P. Role of Mercury Electrodes in Contemporary Analytical Chemistry. *Electroanalysis* **2000**, *12*, 1187–1194. [[CrossRef](#)]
2. Syversen, T.; Kaur, P. Die Toxikologie des Quecksilbers und seiner Verbindungen. *Perspect. Med.* **2014**, *2*, 133–150. [[CrossRef](#)]
3. Regulation (EU) 2017/852 of the European Parliament and of the Council of 17 May 2017 on mercury, and repealing Regulation (EC) No 1102/2008. *OJ L* **2017**, *137*, 1–21.
4. United Nations Environment Program. *Minamata Convention on Mercury: Text and Annexes*; United Nations Environment Programme: Nairobi, Kenya, 2019.
5. Wang, J.; Lu, J.; Hocevar, S.; Farias, P.A.M.; Ogorevc, B. Bismuth-coated carbon electrodes for anodic stripping voltammetry. *Anal. Chem.* **2000**, *72*, 3218–3222. [[CrossRef](#)] [[PubMed](#)]
6. Jovanovski, V.; Hocevar, S.B.; Ogorevc, B. Bismuth electrodes in contemporary electroanalysis. *Curr. Opin. Electrochem.* **2017**, *3*, 114–122. [[CrossRef](#)]
7. Wang, J. Stripping Analysis at Bismuth Electrodes: A Review. *Electroanalysis* **2005**, *17*, 1341–1346. [[CrossRef](#)]
8. Švancara, I.; Prior, C.; Hocevar, S.B.; Wang, J. A Decade with Bismuth-Based Electrodes in Electroanalysis. *Electroanalysis* **2010**, *22*, 1405–1420. [[CrossRef](#)]
9. Hocevar, S.B.; Wang, J.; Deo, R.P.; Ogorevc, B. Potentiometric Stripping Analysis at Bismuth-Film Electrode. *Electroanalysis* **2002**, *14*, 112–115. [[CrossRef](#)]
10. Bedin, K.C.; Mitsuyasu, E.Y.; Ronix, A.; Cazetta, A.L.; Pezoti, O.; Almeida, V.C. Inexpensive Bismuth-Film Electrode Supported on Pencil-Lead Graphite for Determination of Pb(II) and Cd(II) Ions by Anodic Stripping Voltammetry. *Int. J. Anal. Chem.* **2018**, *2018*, 1473706. [[CrossRef](#)]
11. Korolczuk, M.; Rutyna, I.; Tyszczyk, K. Adsorptive Stripping Voltammetry of Nickel at an In Situ Plated Bismuth Film Electrode. *Electroanalysis* **2010**, *22*, 1494–1498. [[CrossRef](#)]
12. Hutton, E.A.; Hocevar, S.B.; Ogorevc, B.; Smyth, M.R. Bismuth film electrode for simultaneous adsorptive stripping analysis of trace cobalt and nickel using constant current chronopotentiometric and voltammetric protocol. *Electrochem. Commun.* **2003**, *5*, 765–769. [[CrossRef](#)]
13. Wang, J. Bismuth film electrodes for adsorptive stripping voltammetry of trace nickel. *Electrochem. Commun.* **2000**, *2*, 390–393. [[CrossRef](#)]
14. Locatelli, C. Platinum, Rhodium, Palladium and Lead: Elements Linked to Vehicle Emissions. Their Simultaneous Voltammetric Determination in Superficial Water. *Electroanalysis* **2005**, *17*, 140–147. [[CrossRef](#)]
15. Melucci, D.; Locatelli, C. Platinum(II), palladium(II), rhodium(III) and lead(II) voltammetric determination in sites differently influenced by vehicle traffic. *Ann. Chim.* **2007**, *97*, 373–384.
16. Wang, X.; Kumar, R.; Myers, D.J. Effect of Voltage on Platinum Dissolution. *Electrochem. Solid-State Lett.* **2006**, *9*, A225. [[CrossRef](#)]
17. Yasuda, K.; Taniguchi, A.; Akita, T.; Ioroi, T.; Siroma, Z. Platinum dissolution and deposition in the polymer electrolyte membrane of a PEM fuel cell as studied by potential cycling. *Phys. Chem. Chem. Phys.* **2006**, *8*, 746–752.
18. Shao, Y.; Yin, G.; Gao, Y. Understanding and approaches for the durability issues of Pt-based catalysts for PEM fuel cell. *J. Power Sources* **2007**, *171*, 558–566. [[CrossRef](#)]
19. Yousfi-Steiner, N.; Moçotéguy, P.; Candusso, D.; Hissel, D. A review on polymer electrolyte membrane fuel cell catalyst degradation and starvation issues: Causes, consequences and diagnostic for mitigation. *J. Power Sources* **2009**, *194*, 130–145.
20. Meier, J.C.; Galeano, C.; Katsounaros, I.; Topalov, A.A.; Kostka, A.; Schüth, F.; Mayrhofer, K.J.J. Degradation Mechanisms of Pt/C Fuel Cell Catalysts under Simulated Start–Stop Conditions. *ACS Catal.* **2012**, *2*, 832–843. [[CrossRef](#)]
21. Borup, R.L.; Kusoglu, A.; Neyerlin, K.C.; Mukundan, R.; Ahluwalia, R.K.; Cullen, D.A.; More, K.L.; Weber, A.Z.; Myers, D.J. Recent developments in catalyst-related PEM fuel cell durability. *Curr. Opin. Electrochem.* **2020**, *21*, 192–200.
22. Javed, H.; Knop-Gericke, A.; Mom, R.V. Structural Model for Transient Pt Oxidation during Fuel Cell Start-up Using Electrochemical X-ray Photoelectron Spectroscopy. *ACS Appl. Mater. Interfaces* **2022**, *14*, 36238–36245. [[CrossRef](#)] [[PubMed](#)]
23. Xu, H.; Kunz, R.; Fenton, J.M. Investigation of Platinum Oxidation in PEM Fuel Cells at Various Relative Humidities. *Electrochem. Solid-State Lett.* **2007**, *10*, B1. [[CrossRef](#)]
24. Nguyen, H.L.; Han, J.; Nguyen, X.L.; Yu, S.; Goo, Y.-M.; Le, D.D. Review of the Durability of Polymer Electrolyte Membrane Fuel Cell in Long-Term Operation: Main Influencing Parameters and Testing Protocols. *Energies* **2021**, *14*, 4048. [[CrossRef](#)]
25. Ehelebe, K.; Knöppel, J.; Bierling, M.; Mayerhöfer, B.; Böhm, T.; Kulyk, N.; Thiele, S.; Mayrhofer, K.J.J.; Cherevko, S. Platinum Dissolution in Realistic Fuel Cell Catalyst Layers. *Angew. Chem. Int. Ed.* **2021**, *60*, 8882–8888. [[CrossRef](#)]
26. Cherevko, S.; Keeley, G.P.; Geiger, S.; Zeradjanin, A.R.; Hodnik, N.; Kulyk, N.; Mayrhofer, K.J.J.; Dissolution of Platinum in the Operational Range of Fuel Cells. *ChemElectroChem* **2015**, *2*, 1471–1478. [[CrossRef](#)]

27. Xie, J.; Wood, D.L.; Wayne, D.M.; Zawodzinski, T. A.; Atanassov, P.; Borup, R. L. Durability of PEFCs at High Humidity Conditions. *J. Electrochem. Soc.* **2005**, *152*, A104. [[CrossRef](#)]
28. Xie, J.; Wood, D.L.; More, K.L.; Atanassov, P.; Borup, R.L. Microstructural Changes of Membrane Electrode Assemblies during PEFC Durability Testing at High Humidity. *J. Electrochem. Soc.* **2005**, *152*, A1011. [[CrossRef](#)]
29. León, C.; Emons, H.; Ostapczuk, P.; Hoppstock, K. Simultaneous ultratrace determination of platinum and rhodium by cathodic stripping voltammetry. *Anal. Chim. Acta* **1997**, *356*, 99–104. [[CrossRef](#)]
30. Metrohm. Determination of Platinum and Rhodium in the Ultratrace Range by Adsorptive Stripping Voltammetry. Application Bulletin 220/ e. 2000. Available online: <https://www.metrohm.com/en/applications/ab-application-bulletins/ab-220.html> (accessed on 18 September 2022).
31. Kolpakova, N.A.; Oskina, Y.A.; Sabitova, Z.K. Determination of Rh(III) by stripping voltammetry on a graphite electrode modified with lead. *J. Solid State Electrochem.* **2018**, *22*, 1933–1939. [[CrossRef](#)]
32. Egoshina, A.V.; Kolpakova, N.A. Determination of Platinum and Rhodium by Stripping Voltammetry. *J. Anal. Chem.* **2021**, *76*, 1435–1437. [[CrossRef](#)]
33. Ustinova, E.M.; Gorchakov, E.V. Comparative Characteristics of Voltammetric Methods Determination of Platinum in Mineral Raw Materials. *Key Eng. Mater.* **2016**, *685*, 739–742. [[CrossRef](#)]
34. van der Horst, C.; Silwana, B.; Iwuoha, E.; Somerset, V. Stripping voltammetric determination of palladium, platinum and rhodium in freshwater and sediment samples from South African water resources. *J. Environ. Sci. Health Part A* **2012**, *47*, 2084–2093. [[CrossRef](#)]
35. Silwana, B.; van der Horst, C.; Iwuoha, E.; Somerset, V. Screen-printed carbon electrodes modified with a bismuth film for stripping voltammetric analysis of platinum group metals in environmental samples. *Electrochim. Acta* **2014**, *128*, 119–127. [[CrossRef](#)]
36. Marotta, A.; Pavlovic, J.; Ciuffo, B.; Serra, S.; Fontaras, G. Gaseous Emissions from Light-Duty Vehicles: Moving from NEDC to the New WLTP Test Procedure. *Environ. Sci. Technol.* **2015**, *49*, 8315–8322. [[CrossRef](#)] [[PubMed](#)]
37. Locatelli, C. Possible interference in the sequential voltammetric determination at trace and ultratrace concentration level of platinum group metals (PGMs) and lead. *Electrochim. Acta* **2006**, *52*, 614–622. [[CrossRef](#)]
38. Elio, D.; Brunetti, B.; Cattaneo, R. Validation of a procedure for quantifying platinum at sub- $\mu\text{g/L}$ level in matrices of alimentary and environmental concern by catalytic adsorptive stripping voltammetry. *J. Phys. IV France* **2003**, *107*, 373–375.
39. Baldrianova, L.; Svancara, I.; Vlcek, M.; Economou, A.; Sotiropoulos, S. Effect of Bi(III) concentration on the stripping voltammetric response of in situ bismuth-coated carbon paste and gold electrodes. *Electrochim. Acta* **2006**, *52*, 481–490. [[CrossRef](#)]
40. Van der Linden, W.E.; Dieker, J.W. Glassy carbon as electrode material in electro-analytical chemistry. *Anal. Chim. Acta* **1980**, *119*, 1–24. [[CrossRef](#)]
41. Cobelo-García, A.; Santos-Echeandía, J.; López-Sánchez, D.E.; Almécija, C.; Omanović, D. Improving the voltammetric quantification of ill-defined peaks using second derivative signal transformation: example of the determination of platinum in water and sediments. *Anal. Chem.* **2014**, *86*, 2308–2313. [[CrossRef](#)]